



HHS Public Access

Author manuscript

Cell Mol Neurobiol. Author manuscript; available in PMC 2017 April 01.

Published in final edited form as:

Cell Mol Neurobiol. 2016 April ; 36(3): 313–325. doi:10.1007/s10571-015-0269-4.

Environmental Enrichment Stimulates Immune Cell Secretion of Exosomes That Promote CNS Myelination and May Regulate Inflammation

Kae M. Pusic^{#1}, Aya D. Pusic^{#1,2}, and Richard P. Kraig^{1,2,*}

¹Department of Neurology The University of Chicago Chicago, IL 60637, USA

²Committee on Neurobiology The University of Chicago Chicago, IL 60637, USA

These authors contributed equally to this work.

Abstract

Environmental enrichment (EE) consists of increased physical, intellectual and social activity, and has wide-ranging effects, including enhancing cognition, learning and memory, and motor coordination. Animal studies have demonstrated that EE improves outcome of brain trauma and neurodegenerative disorders, including demyelinating diseases like multiple sclerosis, making it a promising therapeutic option. However, the complexity of applying a robust EE paradigm makes clinical use difficult. A better understanding of the signaling involved in EE-based neuroprotection may allow for development of effective mimetics as an alternative. In prior work, we found that exosomes isolated from the serum of rats exposed to EE impact CNS myelination. Exosomes are naturally occurring nanovesicles containing mRNA, miRNA, and protein, which play important roles in cell function, disease, and immunomodulation. When applied to hippocampal slice cultures or nasally administered to naïve rats, EE serum exosomes significantly increase myelin content, oligodendrocyte precursor (OPC) and neural stem cell levels, and reduce oxidative stress. We found that rat EE exosomes were enriched in miR-219, which is necessary and sufficient for OPC differentiation into myelinating cells. Thus, peripherally produced exosomes may be a useful therapy for remyelination. Here, we aim to better characterize the impact of EE on CNS health and to determine the cellular source of nutritive exosomes found in serum. We found that exosomes isolated from various circulating immune cell types all increased slice culture myelin content, contained miR-219, and reduced oxidative stress, suggesting that EE globally alters immune function in a way that supports brain health.

Keywords

neuroimmune; hippocampal slice culture; remyelination; multiple sclerosis; aging

*Correspondence should be addressed to (rkraig@neurology.bsd.uchicago.edu), Tel: 773-702-0802; Fax: 773-702-5175 .

Conflict of Interest

The authors report a patent pending entitled, “Exosomes-Based Therapeutics Against Neurodegenerative Disorders” that involves exosomes containing microRNA that promote myelination and prevent spreading depression.

INTRODUCTION

Environmental enrichment (EE) is defined as volitionally increased physical, social and intellectual activity. EE enhances memory, increases production of myelin at all ages, and lessens injury from neurodegenerative disorders including demyelinating disease (Fields 2008). Although most studies of EE have been carried out in rodents, it has been effective in a variety of other animals, including fish, rabbits, farm animals, and non-human primates (Singhal et al., 2014). To date, these studies have shown the effectiveness of EE on a number of CNS diseases, such as Huntington's disease (van Dellen et al., 2000), Alzheimer's disease (Jankowsky et al., 2005), traumatic brain injury (Passineau et al., 2001), and migraine (Darabaneanu et al., 2011). While these types of studies are more difficult to conduct in human patients, there is significant evidence that EE can produce similar results in humans as well.

Increased physical exercise, a form of EE, has been linked to improved outcome for neurological disease, including depression (Strohle, 2009), schizophrenia (Beebe et al., 2005), epilepsy (Arida et al., 2010) and migraine (Varkey et al., 2011). Likewise, there have been numerous studies examining the role of intellectual enrichment in creating 'cognitive reserve' and lessening the impact of brain disease on cognitive impairment (Stern, 2012; Crescentini et al., 2014). Reports also show how social engagement and an active lifestyle can protect against dementia (Fratiglioni et al., 2004) Taken together, these works provide evidence suggesting that EE has a beneficial impact on human brain health.

Though enrichment paradigms vary, they can be broadly characterized as the following types: 1. Social enrichment, in which subjects are given increased exposure to conspecifics (i.e. group housing). 2. Cognitive enrichment, which includes exposure to novel stimuli and experiential learning (i.e. toys and mazes). 3. Physical enrichment, consisting of voluntary exercise (i.e., access to a running wheel). Our EE paradigm provides elements of all three categories of enrichment (detailed in Materials and Methods).

In recent years, there has been increased attention to the development of EE-mimetics (McOmish and Hannan, 2007). To this end, we have studied the role of exosomes in EE, and found that exosomes derived from serum of EE rats increased oligodendrocyte precursor (OPC) numbers, differentiation and myelin production, and also improved remyelination following lysolecithin-induced demyelination in brain slice cultures. Furthermore, aging animals exposed to EE also produced pro-myelinating exosomes, suggesting that EE can restore the ability to produce these exosomes, which is normally diminished in aging animals (Pusic and Kraig 2014). We found that this feature of peripheral exosomes involved miR-219, which is required for production of myelinating oligodendrocytes via regulation of multiple mRNA targets in their differentiation pathway (Dugas et al. 2010; Zhao et al. 2010).

Here, we aimed to determine the cellular source of pro-myelinating exosomes in EE. Since age-related decrease in remyelination is associated with immunosenescence, and the beneficial effects of EE on immune function are well-documented (De la Fuente and Gimenez-Llort 2010), we chose to focus on circulating immune cells.

MATERIALS AND METHODS

Animal use and environmental enrichment

Animal procedures were approved by the University of Chicago Animal Care and Use Committee, and were conducted in accordance with the guidelines published in the Guide for Care and Use of Laboratory Animals (2011). Wistar rats were obtained from Charles River Laboratories.

For EE, twelve male Wistar rats (initial weight ~125 g) were group housed in a two-layered, 58 cm wide, 88 cm long, and 65 cm Marlau-style cage (Obiang et al. 2011; Fares et al. 2013). The bottom layer of the cage consisted of a running wheel for exercise, a resting area, and *ad libitum* access to food and water. The top layer of the cage contained a maze which was changed three times a week, with six variations of the maze used in rotation. Rats climbed from the bottom to the top layer via ramps, progressed through the maze, and descended down another set of ramps to access food and through one-way doors to return back to the exercise and socialization area. Sufficient space was provided to prevent the emergence of dominant male behavior (Marashi et al. 2003). EE rats were housed in this Marlau-style cage for 35 days, with twelve aged-matched non-enriched (NE) rats single-housed under standard conditions.

At the conclusion of EE/NE exposure, animals were anesthetized with progressive exposure to 100% carbon dioxide (i.e., at a rate of 10-30% of the euthanasia chamber volume/minute). Carbon dioxide exposure was continued for a minute after respiratory arrest before animals were decapitated and truncal blood harvested. Brains were harvested and frozen for staining. Spleens and lymph nodes were dissected out after truncal blood collection and processed as described below.

Alternatively for electron microscopy (EM) imaging of cortical myelin, animals were initially anesthetized with 5% isoflurane in oxygen and then given an intraperitoneal injection of ketamine/xylazine while breathing room air. When fully anesthetized, animals were euthanized by intracardiac perfusion first with saline followed by fixative (Pusic and Kraig 2014).

Electron microscopy

Myelin thickness was measured from frontal neocortex. Images were acquired using the University of Chicago Electron Microscopy Core Facility, and g ratios (axon diameter/fiber diameter) quantified using ImagePro software (v.4.5.0.19, Media Cybernetics) (Guy et al. 1991; Chomiak et al. 2009).

FluoroMyelin staining

EE and NE brains were sectioned (14 μ m) using a cryostat (Leica), fixed in 10% buffered formalin phosphate (ThermoFisher Scientific) for 15 minutes, and incubated with FluoroMyelin (1:300; Invitrogen) for 40 minutes to stain myelin (Dugas et al. 2010). FluoroMyelin intensity was quantified using computer-based digital imaging strategies to

assess integrated optical density at defined areas of interest in grey and white matter regions (Pusic and Kraig 2014; Pusic et al. 2014a; Pusic et al. 2015).

Serum sample preparation

For isolation of exosomes from serum of EE and NE animals, truncal blood was collected into sterile 10 mL glass venous blood collection tubes (Becton Dickinson) and incubated at room temperature for at least 20 minutes to allow specimens to clot. Following clot formation, a wooden applicator stick was used to disrupt clot adhesion to the tube wall and samples were centrifuged at $2000 \times g$ for 15 minutes at room temperature. Serum was then transferred to sterile microcentrifuge tubes and stored at -20°C until further processing (Pusic and Kraig 2014).

Isolation of cells from blood, spleen and lymph nodes

Truncal blood from EE/NE animals was collected into sterile heparinized blood collection tubes (Becton Dickinson), inverted several times to avoid blood clotting, and kept at room temperature during subsequent harvests (used within 2 hrs). Anti-coagulated blood was then mixed with an equal volume of cold, calcium-free, magnesium-free Dulbecco's Phosphate-Buffered Saline at pH 7.2 (DPBS; Gibco). 15 mL of Ficoll-Paque PREMIUM (GE Healthcare) was sterilely transferred to a 50 mL tube via syringe, and the diluted blood sample carefully layered on top so as not to disturb the Ficoll interface. The samples were then centrifuged at $400 \times g$ for 30-40 minutes in a swinging bucket set up with free deceleration. 50 mL tubes now contained four discernable layers: 1) Diluted plasma, 2) Peripheral blood mononuclear cells (PBMCs), 3) Ficoll, and 4) Red blood cells / granulocytes. The upper plasma layer was carefully removed and discarded, and the underlying cloudy PBMC layer harvested into clean tubes. PBMCs were then washed in 3x volume of DPBS and centrifuged at $200 \times g$ for ten minutes to pellet cells. Cells were washed once more, then resuspended in 3 mL of DPBS and counted.

Rat spleens or lymph nodes were dissected out and washed with cold DPBS. Tissue was then finely chopped with a razor and crushed through a $40 \mu\text{m}$ cell strainer to obtain a single cell suspension. Cells were then washed twice in cold DPBS (as above), pelleted, resuspended in 3 mL of DPBS and counted. Composition of minimal media is described below.

Specific cell populations were isolated from PBMCs using the Manual MACS Cell Separation platform (Miltenyi Biotec), according to manufacturer's instructions. Briefly, PBMCs were pelleted and resuspended in $90 \mu\text{L}$ per 10^7 cells of cold labeling buffer (DPBS, 0.5% BSA, 2mM EDTA). Cell-specific magnetic beads ($10 \mu\text{L}$ beads per 10^7 cells) were then added to the cell suspension, mixed well, and incubated on ice for 15 min for labeling. Labeled cells were then washed and pelleted as before, and resuspended in labeling buffer (up to 10^8 cells per 500 μL buffer). Finally, cells were run through a magnetic column, followed by a series of wash steps, eluted in 5 mL of labeling buffer, and counted.

All minimal media (see below) were prepared with Exo-Free Fetal Bovine Serum (System Biosciences) and warmed to 37°C before use. Cells were resuspended in appropriate media and at appropriate cell density for that cell type. Cultures were incubated at standard

conditions (36°C, 95% humidity and 5% carbon dioxide-balance air) for three days before conditioned media was collected. Conditioned media was centrifuged at $2000 \times g$ for 15 minutes to remove cell debris, then stored at -20°C for later use or immediately processed for exosome isolation.

Minimal media for cell types were as follows: PBMCs, B cells, T cells: Advanced Minimal Essential Medium (Gibco, Life Science Technologies); 1% MEM vitamin solution; 1% HEPES (1 M); 1% GlutaMAX Supplement; 1% Penicillin-Streptomycin (10,000 U/mL); 0.02% Gentamycin; 10% (all from Gibco Life Science Technologies); 10% Exo-Free Fetal Bovine Serum. Dendritic cells: RPMI-1640 Medium; 1% HEPES (1 M); 25 mM sodium bicarbonate; 10 mM glucose; 1% GlutaMAX Supplement; Penicillin-Streptomycin (10,000 U/mL); 0.02% Gentamycin; 10% (all from Gibco Life Science Technologies); 10% Exo-Free Fetal Bovine Serum; pH 7.4.

Exosome isolation and verification

Exosomes were isolated from rat serum or conditioned media (harvested from cultured blood-derived cell populations) using ExoQuick and ExoQuick-TC respectively (System Biosciences). These products contain different proprietary formulations optimized for the isolation of exosomes from biological fluids (ExoQuick) or from tissue culture medium (ExoQuick-TC). Briefly, 500 μL plasma was mixed with 120 μL ExoQuick solution and incubated at 4°C for 30 minutes, precipitated by centrifugation at $1500 \times g$ for 30 minutes, and resuspended in 100 μL sterile phosphate buffered saline (PBS; 7.3 pH). Conditioned media was mixed with ExoQuick-TC solution (1:5 ratio), and incubated overnight at 4°C . Exosomes were precipitated out of solution by centrifugation at $1500 \times g$ for 30 minutes, and resuspended in 700 μL PBS or lysed for RNA or protein extraction. Slice culture treatments consisted of 70-100 μg of exosomes per tissue culture well containing three hippocampal slice cultures (1.2 mL serum-free media). Recovery of exosomes was confirmed via Western blot analysis of two well-characterized exosomal protein markers, CD63 and Alix. The exosome pellet from 5 mL media was resuspended in 200 μL cold lysis buffer for protein extraction (yield $\sim 700 \mu\text{g}$). Immunoblots for CD63 and Alix (AbD Serotec) were performed as described below. Exosome verification by Western blot could not be performed for all sample types due to small sample sizes, but was performed on representative samples. For all experiments utilizing a specific source of exosomes (i.e., PBMC exosomes or T cell exosomes), samples were representative of pooled cells from 3 or more animals.

Slice culture preparation and use

Hippocampal slice cultures were prepared from P10 Wistar rats. Methods of slice culture preparation, maintenance and experimental manipulations are detailed elsewhere (Pusic et al. 2011). We use hippocampal slice cultures, as this preparation allows for accurate control of microenvironmental conditions over extended periods of time (Grinberg et al. 2012, 2013; Pusic and Kraig 2014; Pusic et al. 2014a; Pusic et al. 2015).

Briefly, untimed pregnant Wistar female rats (Charles River Laboratories) were single-housed with EnviroDri paper bedding (Shepherd Specialty Paper) and Nestlets (Ancare).

Litters were culled to ten pups to reduce variation in pup size. 350 μm slices were prepared from P10 pups of either sex. Slice cultures were initially maintained in a horse serum-based medium and transferred to serum-free medium at 18 days *in vitro* (Pusic et al. 2011). When mature at 21 days *in vitro*, culture vitality was assessed using a dead cell marker, Sytox (Invitrogen), and slices showing significant cell death were discarded (Kunkler et al. 1997; Hulse et al. 2008).

Lipopolysaccharide challenge

Lipopolysaccharide (LPS) derived from *Escherichia coli* O26:B5 was purchased from Sigma-Aldrich. Naïve slice cultures were pre-treated with 70-100 μg exosomes or sterile PBS (control) for three hours before addition of 2 $\mu\text{g}/\text{mL}$ LPS for 24 hours. Following incubation with LPS, cultures were fixed in cold 10% buffered formalin phosphate (ThermoFisher Scientific) for subsequent staining and conditioned media was collected for determination of cytokine content. All samples were stored at -80°C until further processing.

Immunoblotting

Slice culture myelin basic protein (MBP) content was determined as a measure of myelination, using standard SDS-PAGE immunoblotting procedures. 20 μg of total protein from exosome-treated hippocampal slice culture homogenates were loaded to SDS-PAGE gels for separation, transferred to PVDF membranes, and immunolabeled for MBP (Novus Biologicals) with β -actin (Sigma-Aldrich) as a loading control. Blots were visualized by standard chemiluminescence and densitometric quantification was performed utilizing Quantity One 1-D Analysis Software (Bio-Rad). 21.5, 18.5, and 17.2 kDa bands were quantified.

Immunohistochemistry

Hippocampal slice cultures were fixed in 10% buffered formalin phosphate (ThermoFisher Scientific) overnight at 4°C and stained for glial fibrillary acidic protein (GFAP), which is considered a marker of astrogliosis (Brahmachari et al. 2006). Staining procedures followed standard protocols. Briefly, cultures were incubated in blocking buffer [PBS; 0.02% tween 20 (Sigma-Aldrich); 5% goat serum (Life Technologies)] for one hour at room temperature. Primary anti-GFAP antibody (Santa Cruz Biotechnology) was used at 1:1000, and staining was allowed to proceed overnight at 4°C . Cultures were then washed 3x in PBS supplemented with 0.02% tween, and incubated with goat anti-mouse Alexa Fluor-488 (1:1000; Life Technologies) for one hour at room temperature. Finally, cultures were mounted on gel-coated slides with ProLong Gold Antifade mountant (Life Technologies). Staining intensity was quantified as above for FluoroMyelin.

miRNA extraction and profiling

Total RNA was extracted from isolated blood-cell exosomes using mirVana RNA Isolation Kits (Life Technologies) according to manufacturer's instructions. Purity and yield was assessed by NanoDrop. RNA (100 ng) was then reverse transcribed into cDNA using TaqMan MicroRNA Reverse Transcriptase Kits (Life Technologies) and further amplified

with Megaplex PreAmp Primers (Rodent Pool set) with TaqMan PreAmp Master Mix Kits (Life Technologies). Samples were then run on TaqMan Array Rodent MicroRNA A+B Cards Set v3.0 (Life Technologies) on a 7900HT Real-Time PCR System (Life Technologies) (Pusic and Kraig, 2014; Pusic et al., 2014a).

Enzyme-linked immunosorbent assay

Conditioned media from LPS-challenged slice cultures (with or without exosome pre-treatment) were screened utilizing a commercially available ELISA kit (Rat Inflammatory Cytokines Multi-Analyte ELISArray Kit; SABiosciences) according to manufacturer's directions. Cytokines measured by this array are: IL-1 α , IL-1 β , IL-2, IL-4, IL-6, IL-10, IL-12, IL-13, IFN γ , TNF α , GM-CSF and RANTES. Briefly, conditioned media samples were incubated in 12 well strips precoated with cytokine capture antibodies for two hours, washed, then incubated with biotin-conjugated secondary antibodies for 30 minutes. Avidin-HRP was added for colorimetric quantification of bound antibodies (at OD 450).

Measurement of oxidative stress

Oxidative stress (OS) was measured using CellROX Deep Red Reagent (1:1000; Invitrogen), a cell-permeant dye that fluoresces when oxidized by reactive oxygen species. Though CellROX used on its own would provide a readout of baseline oxidative status in exosome-treated slice cultures, here we applied an exogenous stressor to determine what effect exosome treatment has on a slice culture's response to increased oxidative load (i.e., as occurs with inflammation). Menadione exposure (8.6 μ g/mL; Supelco Analytical) was used to generate reactive oxygen species, and resultant CellROX fluorescence measured to determine the relative oxidative tolerance of slice cultures treated with exosomes versus those subjected to menadione alone. Staining intensity was quantified as above for FluoroMyelin.

Data handling and statistics

Data were analyzed using SigmaPlot software (v.12.5; Systat Software). All data were subject to normality testing (p -value to reject: 0.05), equal variance testing (p -value to reject: 0.05), and power ($1-\beta$: > 0.8). For gene expression data (both mRNA and miRNA), fold changes of greater than two were considered significant (Pfaffl 2001). Control groups for each experiment are described in the Results and Figure legends. Controls in each experiment were set to 1.0 with experimental data scaled proportionally to better allow inter-experiment comparisons. Molecular biological data included two technical replicates per experimental measurement. All experimental groups consisted of biological replicates of n 3.

RESULTS

EE increases CNS myelination

Exposure to EE improves CNS myelination in aging animals (Zhao et al. 2012; Yang et al. 2013). Here, we extend this effect in adult rats via measurement of neocortical (grey matter) myelin g ratios from EM images, and FluoroMyelin staining of compact myelin in both white and grey matter. Rats exposed to EE had significantly improved grey matter g ratios

compared to non-enriched (NE) rats. Specific values are: NE: 0.77 ± 0.01 ; EE: 0.69 ± 0.01 (10 images per animal, $n = 3$ animals/group) (Fig. 1). EE brains also showed significantly increased FluoroMyelin staining in both grey (Specific values: NE: 1.00 ± 0.48 ; EE: 5.44 ± 0.08) matter regions (Fig. 1B) and white (Specific values: NE: 1.00 ± 0.16 ; EE: 3.18 ± 0.34) matter regions (Fig. 1C) (10 images per animal, $n = 3$ animals/group).

To better understand what processes are affected by EE to induce neuroprotection and increase myelination, we performed miRNA expression profiling to examine differential miRNA expression in NE versus EE brain tissue. We were especially interested in determining whether CNS levels of miR-219 (a key component of EE-serum exosomes) were increased. Indeed, we found significantly higher (> 2 fold) expression of miR-219 in the brains of EE animals compared to levels in NE animals (Fig. 2). However, the relative increase of miR-219 in EE versus NE brain tissue was notably less than the relative increase of miR-219 in EE versus NE serum exosomes (Pusic and Kraig, 2014; adapted in Fig. 5). This emphasizes the importance of peripheral signaling in EE-based neuroprotection.

Exosomes from EE PBMCs increase slice culture MBP

As a preliminary step in determining the cellular source of pro-myelinating exosomes, we first isolated peripheral blood mononuclear cells (PBMCs) from whole blood of EE and NE animals. PBMCs were briefly cultured in minimal media, which was collected three days later for isolation of PBMC-derived exosomes. These exosomes were then applied to naïve slice cultures (100 μ g) and MBP content assessed three days later. This paradigm was previously used (Pusic and Kraig 2014; Pusic et al. 2014a) in experiments determining the impact of exosomes on myelination. Here we use it as a means to quickly screen for nutritive exosomes, since our sample amount is limited.

EE-derived PBMC exosomes significantly increased slice MBP content compared to NE-derived PMBC exosomes (Fig. 3). Specific values were: Control: 1.00 ± 0.25 ; NE-PBMC-Exos: 1.24 ± 0.26 ; EE-PBMC-Exos: 1.82 ± 0.12 ($n = 6$ /group). This begins to suggest that pro-myelinating exosomes are produced by circulating immune cells in EE-exposed animals. As we have determined that EE-PBMC-Exos increase MBP whereas NE-PBMC-Exos have no effect, in subsequent experiments focusing on specific cell populations, we will assess the impact of exosomes derived from specific EE cell types on baseline slice culture MBP content (naïve slices).

Exosomes from EE PBMCs contain high levels of miR-219 and other miRNA species that were enriched in EE-serum-derived exosomes

Screening of EE-PBMC-derived exosomal miRNA revealed significant differences between the contents of EE-PBMC-Exos and NE-Serum-Exos. For exosomal miRNA expression profiling, fold changes were measured relative to NE-Serum-Exos. This allows us to compare relative fold changes across all groups to fold changes seen in EE-serum exosomes. EE PBMC-Exos were enriched in a number of miRNAs involved in oligodendrocyte differentiation and myelin production pathways, listed in Figure 3A. Notably, miR-219 was highly enriched (>10 fold) in EE-PBMC-Exos, as it was in EE-serum-derived exosomes, which supports our hypothesis that circulating immune cells are the source of pro-

myelinating exosomes. Enriched anti-inflammatory response miRNAs are shown in Figure 3B. miR-27b, miR-181a, and miR-665 were especially highly enriched (>10 fold). Increased presence of these miRNA species indicates the possibility that PBMC exosomes may also reduce inflammation and OS.

Exosomes from EE spleen cells but not lymph node cells increase slice culture MBP

Since exosomes from EE PBMCs both increased slice culture myelin and contained high levels of miR-219, it is likely that one or more circulating cell types is the source of pro-myelinating exosomes. We next wanted to determine whether other sources of immune cells likewise produced pro-myelinating exosomes. To do this, we examined exosomes derived from total spleen and lymph node cells. We found that exosomes produced by spleen cells isolated from EE animals also produce a significant increase in MBP when applied to slice cultures, whereas exosomes from lymph node cells had no effect. Specific values: Control: 1.00 ± 0.04 ; EE Spleen-Exos: 1.60 ± 0.08 , EE Lymph-Exos: 1.13 ± 0.08 ($n=4$ /group) (Fig. 4, left). Interestingly, miRNA expression profiling did not show increased miR-219 in exosomes from spleen cells (Fig. 4, right). However, miR-27a and b reduce OS and may impact myelin indirectly. Alternatively, additional miRNA species (i.e., miR-138) that impact oligodendrocytes were increased in splenic exosomes and may contribute to increased myelin. miR-9 and miR-138, which enhance maturation and differentiation (Lau et al. 2008; Dugas et al. 2010), and mature species of the miR-17-92 cluster, known to induce OPC proliferation both *in vivo* and *in vitro* (Budde et al. 2010), were all present and/or enriched.

Since we saw a greater relative increase in MBP following treatment with EE PBMC exosomes versus EE Spleen exosomes (see above for specific values), and since EE PBMC exosomes' miRNA profiles more closely matched that of EE serum exosomes, we chose to focus on specific cell populations within circulating PBMCs.

Exosomes from EE blood T cells, B cells and DCs increase MBP

PBMCs were once again harvested from EE animals, and specific subpopulations were isolated utilizing the autoMACs bead-based cell sorting platform. Each cell type was cultured in minimal media for three days, then exosomes harvested. As before, since sample sizes were limited, we utilized slice culture MBP content following exosome exposure as a means of screening for functionality. Exosomes were applied to naïve slice cultures at our usual dose of 100 μ g per insert. Three days later, cultures were collected and processed for immunoblotting. We found that exposure to several sources of blood exosomes significantly increased MBP content, though to different degrees. Specific values: Control: 1.00 ± 0.08 ; EE T cell-Exos: 1.97 ± 0.10 ; EE B cell-Exos: 1.99 ± 0.09 ; EE DCEXos: 1.44 ± 0.04 ; ($n=6-9$) (Fig. 5).

miRNA profiling of exosomes from different EE cell populations

Next, we profiled the miRNA content of exosomes from each cell population that increased MBP in slice cultures. miRNA fold changes were calculated relative to NE serum exosomes and compared to changes seen in prior EE serum exosome versus NE serum exosome studies (Fig. 5). Our aim here was to determine which population of exosome's miRNA

profile most closely matches that of EE serum exosomes and to identify differences in their constituents.

miRNAs involved in oligodendrocyte differentiation and myelin production pathways are shown in column A, and anti-inflammatory response miRNAs are shown in column B. All exosome types examined showed significantly higher content of miR-219 than that found in NE serum-Exos. Though we have not examined its role in EE-based neuroprotection, miR-181a was also present at significantly higher levels in all exosome types profiled. The miR-181 family of miRNAs play a role in the regulation of neuroinflammatory responses from astrocytes. Hutchison and co-workers (2013) show that high expression of miR-181 has an anti-inflammatory effect, whereas its down-regulation (e.g., in response to LPS) contributes to astrogliosis and increased production of pro-inflammatory cytokines. Differences between miRNA content and levels will need to be further explored in future studies.

Exosomes from EE blood T cells, B cells and DCs reduce OS

Several miRNA species involved in regulation of inflammatory responses were detected in EE exosomes. miR-181 was of special interest to us, as it was found in high abundance in most EE cell exosomes profiled, and potentially regulates astrocyte production of both oxidative and pro-inflammatory factors (Hutchison et al. 2013). Thus, as a first step in assessing the neuro-protective potential of EE exosomes, we next explored their effect on oxidative status. We found that treatment with each blood cell-derived exosome type significantly increased oxidative tolerance of slice cultures. Oxidative tolerance was assessed by inducing production of reactive oxygen species (ROS) through exposure to menadione, and measuring the CellROX fluorescence produced by the dye reacting with excess ROS that the culture was unable to scavenge. Administration of exosomes three hours prior to menadione exposure significantly reduced resultant OS, as seen in representative images of CellROX staining (Fig. 6A). Specific values: Control: 1.00 ± 0.02 ; EE-serum-Exos: 0.52 ± 0.03 ; EE-PBMC-Exos: 0.16 ± 0.03 ; EE T cell-Exos: 0.61 ± 0.03 ; EE B cell-Exos: 0.44 ± 0.06 ; EE DC-Exos: 0.37 ± 0.10 ; ($n = 3-12$) (Fig. 6B).

Exosomes from EE PBMCs, T cells, B cells and DCs reduce LPS-induced astrogliosis

Next, we focused on the impact of EE exosomes on astrocyte activation. Slice cultures were exposed to LPS, which leads to immune activation resulting in significant and prolonged astrogliosis. We found that treatment with EE exosomes prior to LPS challenge significantly decreased expression of glial fibrillary acidic protein (GFAP), a cytoskeletal protein that is upregulated in activated astrocytes (Fig. 7A). Specific values: Control: 1.00 ± 0.02 ; LPS: 3.06 ± 0.21 ; EE Serum-Exos: 0.35 ± 0.05 ; EE PBMC-Exos: 0.14 ± 0.05 ; EE T cell-Exos: 1.01 ± 0.25 ; EE B cell-Exos: 0.61 ± 0.19 ; EE DC-Exos: 1.31 ± 0.101 ; ($n = 3-9$) (Fig. 7B).

miR-181 negatively regulates the production of multiple cytokines by astrocytes, suppressing their production in an inflammatory environment. Since Hutchison et al. (2013) demonstrated that knockdown of miR-181 in primary astrocytes enhances LPS-induced production of pro-inflammatory cytokines and conversely, overexpression of miR-181 leads to production of anti-inflammatory cytokines, we collected conditioned media from each

treatment group above to determine whether EE exosomes impacted cytokine production. We screened for a panel of twelve pro- and anti-inflammatory cytokines utilizing a multi-analyte ELISArray kit. No significant changes in cytokine content of conditioned media from LPS challenged versus LPS challenge + Exosome-treated cultures were detected. This lack of detection may be due to low sensitivity of the multi-analyte ELISArray kit. Additionally, our use of slice culture is a more complex environment with multiple cell interactions compared to primary astrocyte cultures used by Hutchison.

DISCUSSION

EE enhances memory, increases production of myelin at all ages, and is an intervention known to lessen injury from neurodegenerative disorders including demyelinating disease (Fields 2008). Additionally, EE has beneficial effects on immune function, and can improve age-related immune dysfunction. Studies have also shown that EE improves chemotaxis of phagocytes and lymphocytes and strengthened their responses to infection (Pedersen and Hoffman-Goetz 2000). EE also reduces oxidative stress in immune cells by increasing antioxidant defenses, which may account for overall improved immune function (Arranz et al. 2010).

As experimental enrichment paradigms vary widely, we first confirmed that our specific paradigm provided adequate enrichment and had an impact on myelination. Indeed, animals exposed to enrichment through our Marlaun-style cage showed significant increase in myelination measured in both grey and white matter brain regions. miRNA expression profiling of brain tissue also revealed a significant increase in miR-219 content, though this was not nearly as high as levels found in EE serum exosomes. However, we would like to point out two notable miRNA species that were enriched in EE brains (Fig. 2). miR-27b is maintained at high levels in the Ames dwarf mouse (a model of longevity) and is thought to contribute to increased life span by reducing cellular oxidative status (Bates et al. 2010). miR-124 is deficient in MS lesions, and is thought to maintain a quiescent microglial phenotype, also reducing the oxidative status of these cells (Ponomarev et al. 2013). Thus neurological benefits of EE may include its local effects on miRNA expression in the brain.

In prior work, we found that exosomes derived from the serum of rats exposed to an EE paradigm improved CNS myelination both *in vitro* and *in vivo*. Though there are many aspects of myelination/remyelination that remain to be studied (i.e., neural stem cell proliferation and stages of oligodendrocyte precursor differentiation), since increased slice culture myelin was a reliable functional endpoint in our previous EE exosome studies, we use it here as a means of determining which cell type(s) are producing myelin-promoting exosomes. We found that multiple immune cell populations derived from EE animals produced exosomes that significantly impacted slice culture myelin.

Encouraged by this finding, we screened exosomal miRNA profiles to determine which cell type(s) may be the source of pro-myelinating exosomes found in EE serum. Though all exosome types screened showed different miRNA profiles, each contained higher levels of one or more miRNA species known to impact myelin production or maintenance. It is important here to note that we focused on exosomal miRNAs based on our prior work with

EE serum exosomes. In that study, we observed that transfecting EE serum exosomes with a specific inhibitor of miR-219 abrogated their impact on myelin, suggesting a key role for miR-219. However, we recognize that these exosomes may contain additional mRNAs and proteins that could contribute to their effects.

Based on the broad beneficial effects of EE on immune function, it is likely that the pro-myelinating effect is not due to a specific cell type, but a common property of many immune cell types. In support of this, we have found that exosomes produced by splenic cells isolated from EE animals also produce a significant increase in myelin basic protein when applied to slice cultures. This increase was not as robust as that seen with blood cell populations. However, since exosomes from non-enriched rat spleen cells had no effect, it suggests that enrichment alters immune function in a way that supports brain health, and does so through changes in multiple immune cell populations.

miRNA expression profiling of exosomes derived from each cell type showed that all blood cell-derived exosomes examined contained miR-219. This supports our finding of increased slice culture myelin from exposure to immune cell-derived exosomes, and suggests miR-219 may be responsible for this effect. However, it is interesting to note which other miRNA species were consistently found in higher levels than in NE serum exosomes. miR-9 and miR-17, which are involved in oligodendrocyte proliferation, and miR181a, which has an anti-inflammatory function, were also highly abundant in a subset of EE exosomes. miR-665 was also present at high levels in several EE exosome types. Though its function is unclear, miR-665 is reduced in patients with temporal lobe epilepsy and may affect brain immune function in a manner that dysregulates neuronal excitability (Kan et al. 2012).

Finally, as a first step in assessing the impact of EE exosomes on homeostatic response to inflammation, we examined their effect on OS and astrogliosis in slice cultures. Astrocytes perform a supportive role in the CNS, including transfer of nutrients and the antioxidant glutathione to adjacent neurons (Allen and Barres 2009). Neurodegenerative diseases, aging, and other conditions that increase oxidative stress can increase astrocyte activation (Salminen et al. 2011; Steel and Robinson 2012). In turn, activated astrocytes are less able to cope with OS and increase their secretion of ROS, making neurons more vulnerable to damage. EE, on the other hand, reduces the impact of CNS oxidative damage (Pusic et al. 2014b). Our results here show that EE-derived exosomes from immune cells significantly impact both oxidative tolerance and astrogliosis.

Additional work will be necessary to determine the effect EE derived exosome subsets on parameters such as inflammation and oligodendrocyte precursor maturation. This may help us determine the role of additional enriched miRNAs and determine what combination of miRNA species from each exosome type may be required for an optimal effect on myelination and oxidative tolerance.

Acknowledgements

This work was supported by the National Institutes of Health Common Fund, through the Office of Strategic Coordination/Office of the Director (3UH2 TR000918-02 and 3UH2 TR000918-02S1), core facilities funds from the National Center for Advancing Translational Sciences of the National Institutes of Health (UL1 TR000430), the National Institute of Neurological Disorders and Stroke (NS-019108), the National Institute of Child Health and

Human Disorders (5PO1 HD-09402). We thank Dr. Lisa Won and Jason Schumer for reading and commenting on the manuscript. We also thank Dr. Y. Chen for assistance with immunostaining and electron microscopy. Electron microscopy was performed at the University of Chicago Electron Microscopy Facility.

REFERENCES AND CITATIONS

- Allen JA, Barres BA. Glia – more than just brain glue. *Nature*. 2009; 457(5):457–677.10.1038/457675a
- Arida RM, Scorza FA, Cavalheiro EA. Favorable effects of physical activity for recovery in temporal lobe epilepsy. *Epilepsia*. 2010; 51(Suppl 3):76–9.10.1111/j.1528-1167.2010.02615.x [PubMed: 20618406]
- Arranz L, De Castro NM, Baeza I, Maté I, Viveros MP, De la Fuente M. Environmental enrichment improves age-related immune system impairment: long-term exposure since adulthood increases life span in mice. *Rejuvenation Research*. 2010; 13(4):415–28.10.1089/rej.2009.0989 [PubMed: 20707722]
- Bates DJ, Li N, Liang R, Sarojini H, An J, Masternak MM, Bartke A, Wang E. MicroRNA regulation in Ames dwarf mouse liver may contribute to delayed aging. *Aging Cell*. 2010; 9(1):1–18.10.1111/j.1474-9726.2009.00529.x [PubMed: 19878148]
- Beebe LH, Tian L, Morris N, Goodwin A, Allen SS, Kuldau J. Effects of exercise on mental and physical health parameters of persons with schizophrenia. *Issues in Mental Health Nursing*. 2005; 26(6):661–76.10.1080/01612840590959551 [PubMed: 16020076]
- Brahmachari S, Fung YK, Pahan K. Induction of glial fibrillary acidic protein expression in astrocytes by nitric oxide. *J Neuroscience*. 2006; 26(18):4930–4939.10.1523/JNEUROSCI.5480-05.2006 [PubMed: 16672668]
- Budde H, Schmitt S, Fitzner D, Opitz L, Salinas-Riester G, Simons M. Control of oligodendroglial cell number by the miR-17-92 cluster. *Development*. 2010; 137(13):2127–32.10.1242/dev.050633 [PubMed: 20504959]
- Chomiak T, Hu B. What is the optimal value of the g-ratio for myelinated fibers in the rat CNS? A theoretical approach. *PloS One*. 2009; 4(11):e7754.10.1371/journal.pone.0007754 [PubMed: 19915661]
- Crescentini C, Urgesi C, Fabbro F, Eleopra R. Cognitive and brain reserve for mind-body therapeutic approaches in multiple sclerosis: A review. *Restorative Neurology and Neuroscience*. 2014;10.3233/RNN-130364
- Darabaneanu S, Overath CH, Rubin D, Luthje S, Sye W, Niederberger U, Weisser B. Aerobic exercise as a therapy option for migraine: a pilot study. *International Journal of Sports Medicine*. 2011; 32(6):455–60.10.1055/s-0030-1269928 [PubMed: 21472632]
- De la Fuente M, Gimenez-Llort L. Models of aging of neuroimmunomodulation: strategies for its improvement. *Neuroimmunomodulation*. 2010; 17(3):213–6.10.1159/000258727 [PubMed: 20134206]
- Dugas JC, Cuellar TL, Scholze A, Ason B, Ibrahim A, Emery B, Barres BA. Dicer1 and miR-219 Are required for normal oligodendrocyte differentiation and myelination. *Neuron*. 2010; 65(5):597–611.10.1016/j.neuron.2010.01.027 [PubMed: 20223197]
- Fares RP, Belmeguenai A, Sanchez PE, Kouchi HY, Bodennec J, Morales A, Bezi L. Standardized environmental enrichment supports enhanced brain plasticity in healthy rats and prevents cognitive impairment in epileptic rats. *PloS One*. 2013; 8(1):e53888.10.1371/journal.pone.0053888 [PubMed: 23342033]
- Fields RD. White matter in learning, cognition and psychiatric disorders. *Trends in Neurosciences*. 2008; 31(7):361–70.10.1016/j.tins.2008.04.001 [PubMed: 18538868]
- Fratiglioni L, Paillard-Borg S, Winblad B. An active and socially integrated lifestyle in late life might protect against dementia. *The Lancet. Neurology*. 2004; 3(6):343–53.10.1016/S1474-4422(04)00767-7 [PubMed: 15157849]
- Grinberg YY, van Drongelen W, Kraig RP. Insulin-like growth factor-1 lowers spreading depression susceptibility and reduces oxidative stress. *Journal of Neurochemistry*. 2012; 122(1):221–9.10.1111/j.1471-4159.2012.07763.x [PubMed: 22524542]

- Grinberg YY, Dibbern ME, Levasseur VA, Kraig RP. Insulin-like growth factor-1 abrogates microglial oxidative stress and TNF- α responses to spreading depression. *Journal of Neurochemistry*. 2013; 126(5):662–72.10.1111/jnc.12267 [PubMed: 23586526]
- Guy J, Ellis EA, Hope GM, Emerson S. Maintenance of myelinated fibre g ratio in acute experimental allergic encephalomyelitis. *Brain : A Journal of Neurology*. 1991; 114(Pt 1):281–94. doi: <http://dx.doi.org/281-294>. [PubMed: 1998887]
- Hulse RE, Swenson WG, Kunkler PE, White DM, Kraig RP. Monomeric IgG is neuroprotective via enhancing microglial recycling endocytosis and TNF-alpha. *Journal of Neuroscience*. 2008; 28(47):12199–211.10.1523/JNEUROSCI.3856-08.2008 [PubMed: 19020014]
- Hutchison ER, Kawamoto EM, Taub DD, Lal A, Abdelmohsen K, Zhang Y, Mattson MP. Evidence for miR-181 involvement in neuroinflammatory responses of astrocytes. *Glia*. 2013; 61(7):1018–28.10.1002/glia.22483 [PubMed: 23650073]
- Jankowsky JL, Melnikova T, Fadale DJ, Xu GM, Slunt HH, Gonzales V, Savonenko AV. Environmental enrichment mitigates cognitive deficits in a mouse model of Alzheimer's disease. *The Journal of Neuroscience : The Official Journal of the Society for Neuroscience*. 2005; 25(21):5217–24.10.1523/JNEUROSCI.5080-04.2005 [PubMed: 15917461]
- Kan AA, van Erp S, Derijck AA, de Wit M, Hessel EV, O'Duibhir E, de Jager W, Van Rijen PC, Gosselaar PH, de Graan PN, Pasterkamp RJ. Genome-wide microRNA profiling of human temporal lobe epilepsy identifies modulators of the immune response. *Cell Mol Life Sci*. 2012; 69(18):3127–3145.10.1007/s00018-012-0992-7 [PubMed: 22535415]
- Kunkler PE, Kraig RP. Reactive astrogliosis from excitotoxic injury in hippocampal organ culture parallels that seen in vivo. *Journal of Cerebral Blood Flow and Metabolism*. 1997; 17(1):26–43.10.1097/00004647-199701000-00005 [PubMed: 8978384]
- Lau P, Verrier JD, Nielsen JA, Johnson KR, Notterpek L, Hudson LD. Identification of dynamically regulated microRNA and mRNA networks in developing oligodendrocytes. *Journal of Neuroscience*. 2008; 28(45):11720–30.10.1523/JNEUROSCI.1932-08.2008 [PubMed: 18987208]
- Marashi V, Barnekow A, Ossendorf E, Sachser N. Effects of different forms of environmental enrichment on behavioral, endocrinological, and immunological parameters in male mice. *Hormones and Behavior*. 2003; 43(2):281–92.10.1016/S0018-506X(03)00002-3 [PubMed: 12694638]
- McOmish CE, Hannan AJ. Enviromimetics: exploring gene environment interactions to identify therapeutic targets for brain disorders. *Expert Opinion on Therapeutic Targets*. 2007; 11(7):899–913.10.1517/14728222.11.7.899 [PubMed: 17614759]
- Obiang P, Maubert E, Bardo I, Nicole O, Launay S, Bezin L, Agin V. Enriched housing reverses age-associated impairment of cognitive functions and tPA-dependent maturation of BDNF. *Neurobiology of Learning and Memory*. 2011; 96(2):121–9.10.1016/j.nlm.2011.03.004 [PubMed: 21440650]
- Passineau MJ, Green EJ, Dietrich WD. Therapeutic effects of environmental enrichment on cognitive function and tissue integrity following severe traumatic brain injury in rats. *Experimental Neurology*. 2001; 168(2):373–84.10.1006/exnr.2000.7623 [PubMed: 11259125]
- Pedersen BK, Hoffman-Goetz L. Exercise and the immune system: regulation, integration, and adaptation. *Physiological Reviews*. 2000; 80(3):1055–81. [PubMed: 10893431]
- Pfaffl MW. A new mathematical model for relative quantification in real-time RT-PCR. *Nucleic Acids Research*. 2001; 29(9):e45.10.1093/nar/2909e45 [PubMed: 11328886]
- Ponomarev ED, Veremeyko T, Weiner HL. MicroRNAs are universal regulators of differentiation, activation, and polarization of microglia and macrophages in normal and diseased CNS. *Glia*. 2013; 61(1):91–103.10.1002/glia.22363 [PubMed: 22653784]
- Pusic AD, Kraig RP. Youth and environmental enrichment generate serum exosomes containing miR-219 that promote CNS myelination. *Glia*. 2014; 62(2):284–99.10.1002/glia.22606 [PubMed: 24339157]
- Pusic AD, Grinberg YY, Mitchell HM, Kraig RP. Modeling neural immune signaling of episodic and chronic migraine using spreading depression in vitro. *Journal of Visualized Experiments : JoVE*. 2011; (52)10.3791/2910

- Pusic AD, Mitchell HM, Kunkler PE, Kraig RP. Spreading depression transiently disrupts myelin via interferon-gamma signaling. *Experimental Neurology*. 2015; 264:43–54. doi.org./10.1016/j.expneurol.2014.12.001. [PubMed: 25500111]
- Pusic AD, Pusic KM, Clayton BLL, Kraig RP. IFN γ -stimulated dendritic cell exosomes as a potential therapeutic for remyelination. *Journal of Neuroimmunology*. 2014a; 266(1-2):12–23.10.1016/j.jneuroim.2013.10.014 [PubMed: 24275061]
- Pusic KM, Pusic AD, Kemme J, Kraig RP. Spreading depression requires microglia and is decreased by their M2a polarization from environmental enrichment. *Glia*. 2014b; 62(7):1176–94.10.1002/glia.22672 [PubMed: 24723305]
- Salminen A, Ojala J, Kaarniranta K, Haapasalo A, Hiltunen M, Soininen H. Astrocytes in the aging brain express characteristics of senescence-associated secretory phenotype. *Eur J Neurosci*. 2011;3–11.10.1111/j.1460-9568.2011.07738x [PubMed: 21649759]
- Singhal G, Jaehne EJ, Corrigan F, Baune BT. Cellular and molecular mechanisms of immunomodulation in the brain through environmental enrichment. *Front Cell Neurosci*. 2014; 8:97.10.3389/fncel.2014.00097 [PubMed: 24772064]
- Steele ML, Robinson SR. Reactive astrocytes give neurons less support: implications for Alzheimer's disease. *Neurobiology of Aging*. 2012; 423:e1–423.e13.10.1016/j.neurobiolaging.2010.09.018 [PubMed: 21051108]
- Stern Y. Cognitive reserve in ageing and Alzheimer's disease. *Lancet Neurology*. 2012; 11(11):1006–12.10.1016/S1474-4422(12)70191-6 [PubMed: 23079557]
- Ströhle A, Stoy M, Graetz B, Scheel M, Wittmann A, Gallinat J, Hellweg R. Acute exercise ameliorates reduced brain-derived neurotrophic factor in patients with panic disorder. *Psychoneuroendocrinology*. 2010; 35(3):364–8.10.1016/j.psyneuen.2009.07.013 [PubMed: 19682803]
- Van Dellen A, Blakemore C, Deacon R, York D, Hannan AJ. Delaying the onset of Huntington's in mice. *Nature*. 2000; 404(6779):721–2.10.1038/35008142 [PubMed: 10783874]
- Varkey E, Cider A, Carlsson J, Linde M. Exercise as migraine prophylaxis: a randomized study using relaxation and topiramate as controls. *Cephalalgia : An International Journal of Headache*. 2011; 31(14):1428–38.10.1177/0333102411419681 [PubMed: 21890526]
- Yang S, Li C, Qiu X, Zhan L, Lu W, Chen L, Zhao YY, Shi XY, Huang CX, Cheng GH, Tang Y. Effects of an enriched environment on myelin sheaths in the white matter of rats during normal aging: A stereological study. *Neuroscience*. 2013; 234:13–21.10.1016/j.neuroscience.2013.01.003 [PubMed: 23313226]
- Zhao X, He X, Han X, Yu Y, Ye F, Chen Y, Lu QR. MicroRNA-mediated control of oligodendrocyte differentiation. *Neuron*. 2010; 65(5):612–26.10.1016/j.neuron.2010.02.018 [PubMed: 20223198]
- Zhao YY, Shi XY, Qi X, Lu W, Yang S, Li C, Tang Y. Enriched environment increases the myelinated nerve fibers of aged rat corpus callosum. *Anatomical Record*. 2012; 295(6):999–1005.10.1002/ar.22446

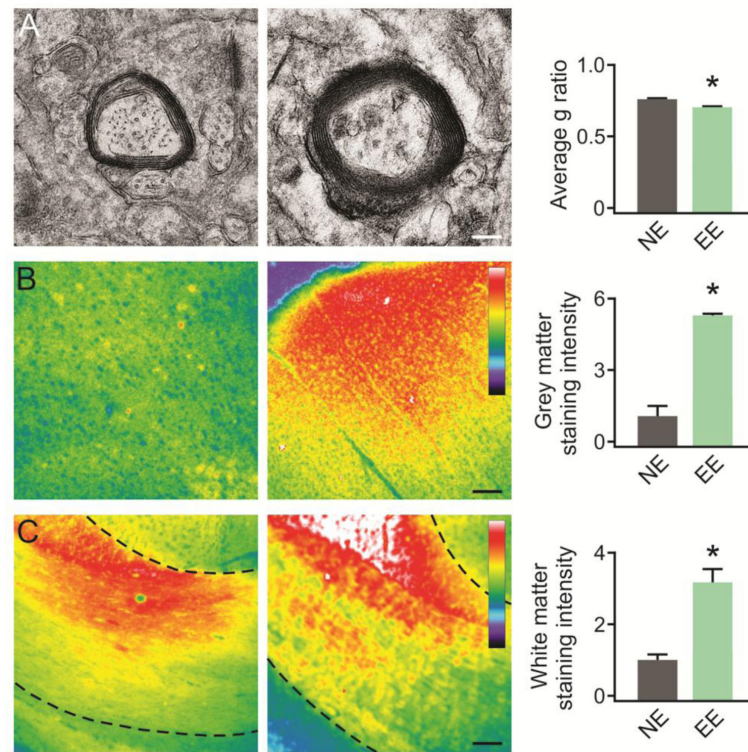


Figure 1.

Environmental enrichment increases CNS myelin. (A) Representative electron micrographs of myelinated axons at the paramedian frontal motor neocortex from non-enriched control (left) and environmentally enriched (right) animals. Scale bar = 200 nm. Myelin g ratios (axon diameter/ myelin sheath diameter) were calculated from electron micrographs. Exposure to environmental enrichment resulted in significantly ($*p = 0.024$) improved g ratios compared to non-enriched, age matched controls. (B-C) Representative images of FluoroMyelin staining, a marker for myelin, in (B) neocortical grey matter and (C) white matter regions of non-enriched (left) and environmentally enriched (right) brains. Scale bars = 100 μm , dotted lines in (C) indicate white matter tract boundaries of the corpus callosum. Quantification of FluoroMyelin intensity showed a significant ($*p = 0.004$) increase in myelin content in (B) white matter, and a significant ($*p = 0.001$) increase in myelin content in (C) grey matter regions. Significance determined by Student's *t*-test.

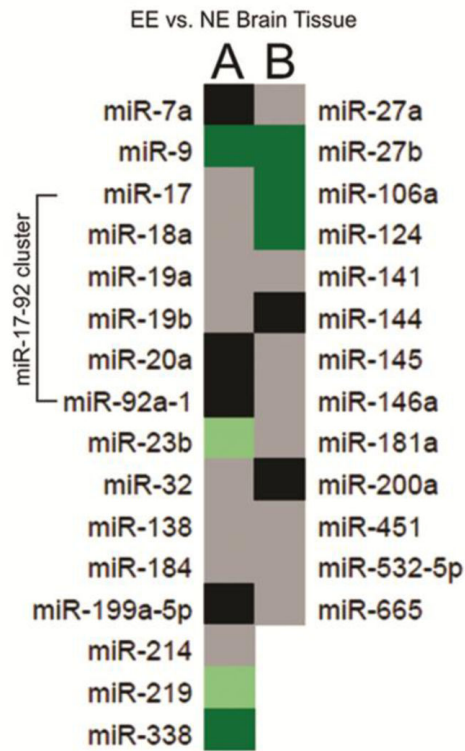
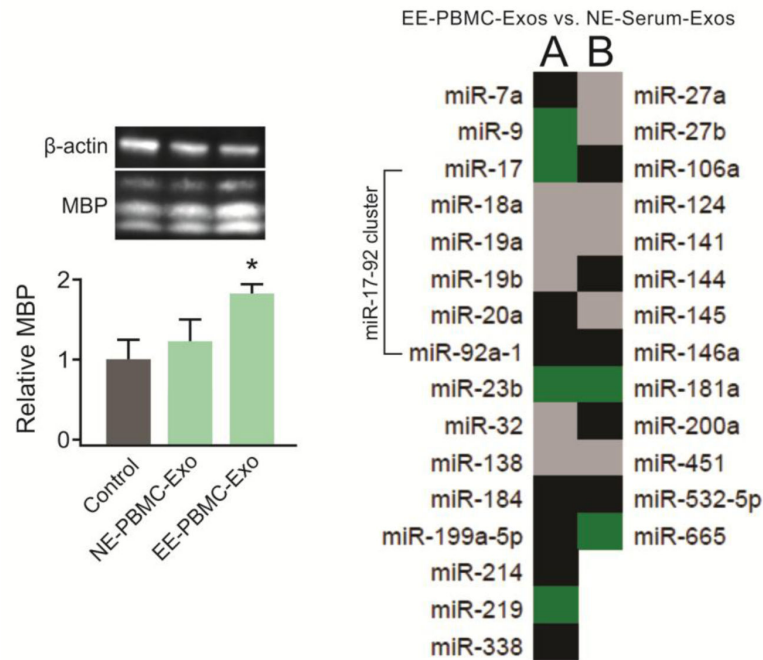


Figure 2.

Differential miRNA expression in EE versus NE rat brains. miRNA content of brain tissue from rats exposed to environmental enrichment was compared to that of age-matched, non-enriched rats. Results show expression levels of specific miRNAs involved in (A) myelin production / oligodendrocyte differentiation and (B) anti-inflammatory response. Black panels indicate mature miRNA species that could not be detected; grey panels indicate miRNAs that were readily detectible but not significantly enriched; light green indicate significantly enriched (i.e., >2 fold) miRNAs; and dark green indicates highly enriched (i.e., >10 fold) miRNAs.

**Figure 3.**

Exosomes produced by peripheral blood mononuclear cells from EE animals increased slice culture myelination, and were enriched in miRNA species involved in myelin production and anti-inflammatory response. Peripheral blood mononuclear cells (PBMCs) were harvested from animals exposed to environmental enrichment (EE) and non-enriched age-matched controls. When applied to hippocampal slice cultures, exosomes from EE PBMCs significantly ($*p < 0.033$) increased MBP levels relative to NE PBMC exosomes and control untreated cultures (left). Significance determined by ANOVA plus post hoc Holm-Sidak testing. miRNA content of EE PBMC-Exos were compared to that of NE total serum-Exos (right). Results show expression levels of specific miRNAs involved in (A) myelin production / oligodendrocyte differentiation and (B) anti-inflammatory response. Black panels indicate mature miRNA species that could not be detected; grey panels indicate miRNAs that were readily detectible but not significantly enriched; light green indicate significantly enriched (i.e., >2 fold) miRNAs; and dark green indicates highly enriched (i.e., >10 fold) miRNAs.

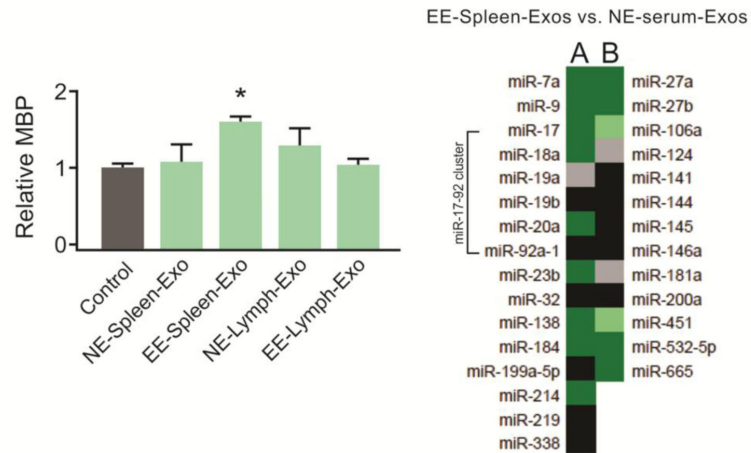


Figure 4.

Exosomes from EE spleen cells increased slice culture myelination, and were enriched in miRNA species involved in myelin production and anti-inflammatory response. Splenic cells and lymph cells were harvested from non-enriched animals (NE) and animals exposed to environmental enrichment (EE) and briefly cultured in exo-free media. When applied to hippocampal slice cultures, only exosomes produced by EE spleen cells significantly ($*p < 0.001$) increased myelin basic protein (MBP) relative to control, untreated cultures. Significance determined by ANOVA plus post hoc Holm-Sidak testing. miRNA profiling results show expression levels of specific miRNAs involved in (A) myelin production / oligodendrocyte differentiation and (B) anti-inflammatory response. Black panels indicate mature miRNA species that could not be detected; grey panels indicate miRNAs that were readily detectable but not significantly enriched; light green indicate significantly enriched (>2 fold); and dark green indicates highly enriched (>10 fold) miRNAs.

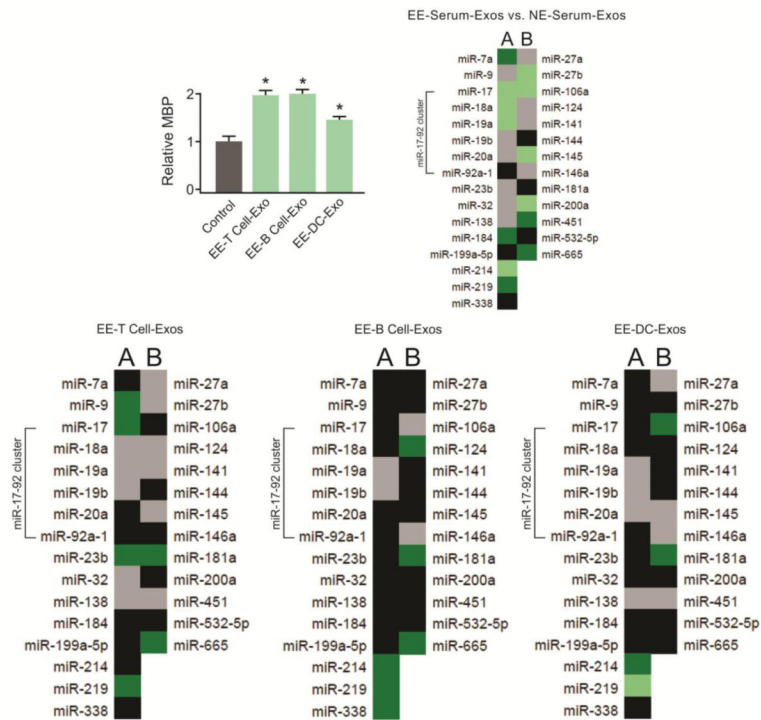


Figure 5.

Exosomes from EE-derived T cells, B cells and blood dendritic cells all increased slice culture myelination, and were enriched in miRNA species involved in myelin production and anti-inflammatory response. PBMCs were harvested from animals exposed to environmental enrichment (EE) as before, then sorted into T cell, B cell and dendritic cell populations. When applied to hippocampal slice cultures, exosomes from all three cell populations significantly ($*p < 0.001$) increased myelin basic protein (MBP) relative to control, untreated cultures. Significance determined by ANOVA plus post hoc Holm-Sidak testing. miRNA expression profiles of EE-derived T cells, B cells and blood dendritic cell exosomes. Expression levels in individual EE blood cell exosomes were calculated relative to that of NE-serum-Exos (from right to left; EE-serum-Exos, EE-T cell-Exos, EE-B cell-Exos and EE-blood DC-Exos). Results show expression levels of specific miRNAs involved in (A) myelin production / oligodendrocyte differentiation and (B) anti-inflammatory response. Black panels indicate mature miRNA species that could not be detected; grey panels indicate miRNAs that were readily detectible but not significantly enriched; light green indicate significantly enriched (i.e., >2 fold) miRNAs; and dark green indicates highly enriched (i.e., >10 fold) miRNAs.

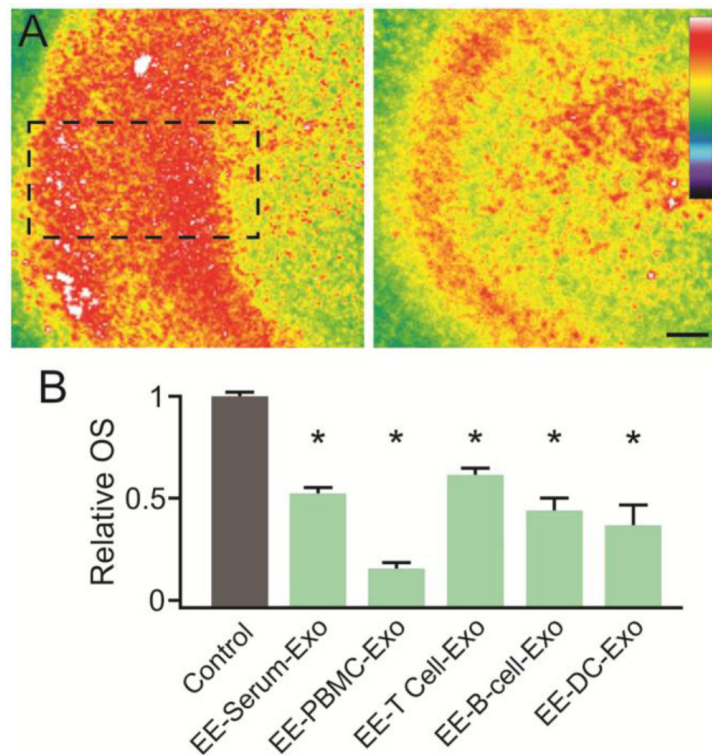


Figure 6.

Exosomes from EE-derived T cells, B cells and blood dendritic cells all increased slice culture oxidative tolerance. (A) Representative images of staining for menadione-induced oxidative stress (CellROX) in control (left) and EE exosome-treated (right) slice cultures. Scale bar = 200 μ m. Dotted line indicates the CA3 region of interest used for quantification. (B) Quantification of CellROX fluorescence at the CA3 region showed a significant ($*p < 0.001$) decrease in oxidative stress following menadione exposure in slice cultures that received EE exosomes versus untreated controls. Significance determined by ANOVA plus post hoc Holm-Sidak testing.

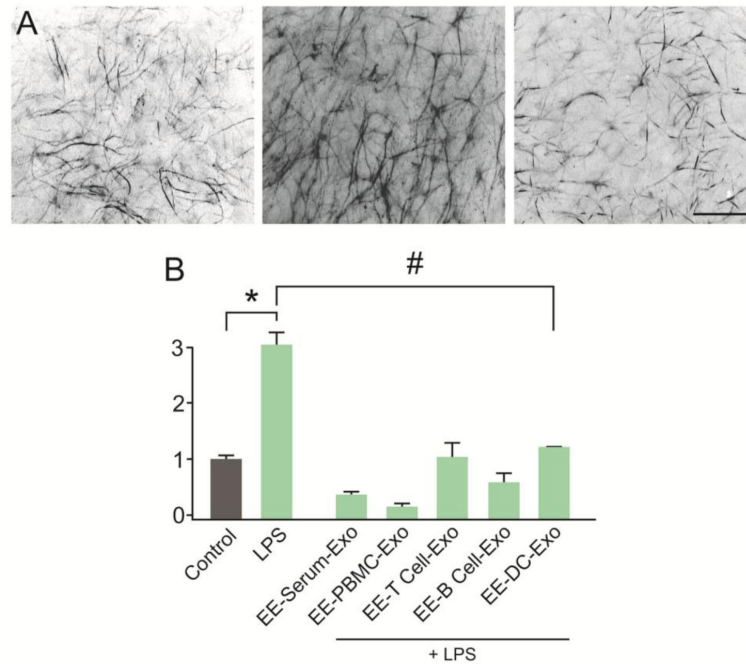


Figure 7.

Exosomes from EE-derived T cells, B cells and blood dendritic cells all reduced astrogliosis from lipopolysaccharide challenge. (A) Representative images of staining for glial fibrillary acidic protein (GFAP) in untreated control (left), lipopolysaccharide (LPS) challenged (middle), and LPS+EE exosome-treated (right) slice cultures. Scale bar = 200 μm . (B) Quantification of staining confirmed a significant ($*p = 0.001$) increase in GFAP positive staining, indicative of astrogliosis, in cultures exposed to LPS. Conversely, there was a significant ($\#p = <0.001$) reduction in astrogliosis in slice cultures treated with EE exosomes following LPS challenge. GFAP staining intensity was not significantly different in LPS+EE exosome-treated cultures and control cultures not exposed to LPS. Significance determined by ANOVA plus post hoc Holm-Sidak testing